Author for correspondence:
M. C. Rodríguez-Uribe,
E-mail: maria.ruribe@academicos.udg.mx

Benthic infauna associated with a shallow-water hydrothermal system of Punta Mita (Mexico)

M. C. Rodríguez-Uribe[1] [ID], F. J. Núñez-Cornú[2], R. M. Prol-Ledesma[3] and P. Salazar-Silva[4]

[1]Departamento de Ciencias Exactas, Centro Universitario de la Costa, Universidad de Guadalajara, Puerto Vallarta, Jalisco 48280, México; [2]C.A. Sismología y Volcanología de Occidente (SisVoc), Centro Universitario de la Costa, Universidad de Guadalajara, Puerto Vallarta, Jalisco 48280, México; [3]Instituto de Geofísica, Universidad Nacional Autónoma de México, Circuito Exterior S/N, 04510, Ciudad de México, México and [4]Tecnológico Nacional de México, Instituto Tecnológico de Bahía de Banderas, Crucero a Punta Mita S/N, 63763, La Cruz de Huanacaxtle, Nayarit, México

Abstract

The shallow-water hydrothermal system of Punta Mita in Banderas Bay is located on the fault called Fisura de las Coronas off Punta Pantoque beach. In this area, three sites with hydrothermal vents were studied at a depth of 9 m. This study aimed to characterize the structure of the benthic infauna communities that coexist in this hydrothermal system; therefore, physico-chemical parameters were measured and the organisms found in the sediment samples were identified up to the class taxonomic level. The highest temperatures (89°C) were recorded within the hydrothermal influence area, which was reflected in an inverse relationship with pH, conductivity and salinity. Sediment temperature profiles increased at greater depth. A total of 371 individuals were found and these were grouped into eight classes: Malacostraca, Maxillopoda, Gastropoda, Bivalvia, Scaphopoda, Polychaeta, Leptocardii and Stenolaemata. The Malacostraca class was the most abundant with 240 individuals, while the Scaphopoda was the lowest with 3. The organic matter contents in the sediments were higher in the areas adjacent to the hydrothermal activity. The high temperature of the hydrothermal discharges structures the benthic community since it was the factor that differed most significantly in the study sites, causing lower abundances in the area of hydrothermal influence compared with the more distant areas. Despite the above, it is concluded that the benthic community of the area with hydrothermal activity is part of the community adjacent to this influence, only in lower numbers.

Introduction

Based on their depth, shallow-water systems are those that occur at depths less than 200 m (Prol-Ledesma *et al.*, 2005; Tarasov *et al.*, 2005). This depth coincides with the maximum depth that the natural light can penetrate in the ocean; although natural light can penetrate deeper under the right conditions, significant light is rarely experienced beyond 200 m (Garrison & Ellis, 2016). Shallow-water hydrothermal systems present a gaseous phase, absent in deep-sea hydrothermal systems (Tarasov *et al.*, 2005), as a result, in the past they were called gasohydrothermal vents (Dando *et al.*, 1995). Most of these hydrothermal systems are associated with volcanic arcs, so the gases are enriched in volcanic volatiles, which causes more acidic fluids and leaching of Mg and other elements, particularly metals, from host rocks (Yang & Scott, 1996; Reeves *et al.*, 2011).

Shallow-water hydrothermal systems are also characterized by very low hydrogen sulphide (H_2S) concentrations and smooth horizontal temperature gradients that are not as steep as in deep-sea hydrothermal systems, as had been recorded in some submarine hydrothermal systems around islands such as Vulcano (Italy), Ischia (Italy) and Faial (Azores, Portugal), and also in Milne Bay Province (Papua New Guinea) (Price & Giovannelli, 2017). In addition, some shallow-water systems are being used as natural laboratories to study the effects of ocean acidification on biota and microbiota (Hall-Spencer *et al.*, 2008; Fabricius *et al.*, 2011; Engel *et al.*, 2015), since CO_2 and H_2S emissions in shallow hydrothermal systems found in seawater with dissolved oxygen are oxidized to form sulphuric acid (H_2SO_4) and carbonic acid (H_2CO_3), which cause a drop in the pH levels of the seawater adjacent to hydrothermal vents and have been shown to remove or dissolve nearby carbon-secreting organisms, leading to potentially dramatic changes in the coastal marine ecosystem in terms of richness and abundance (Hall-Spencer *et al.*, 2008).

The infauna is better known in shallow-water than in deep-sea systems (Tarasov *et al.*, 2005). It is worth highlighting that nematodes are the common denominator in both systems, and the highest abundances have been reported in shallow systems, such as in a shallow-water hydrothermal system of Milos Island in the Aegean Sea (Thiermann *et al.*, 1994; Dando *et al.*, 1995), and in the Kraternaya Bight on the Kuril Islands in the Russian Federation (Tarasov,
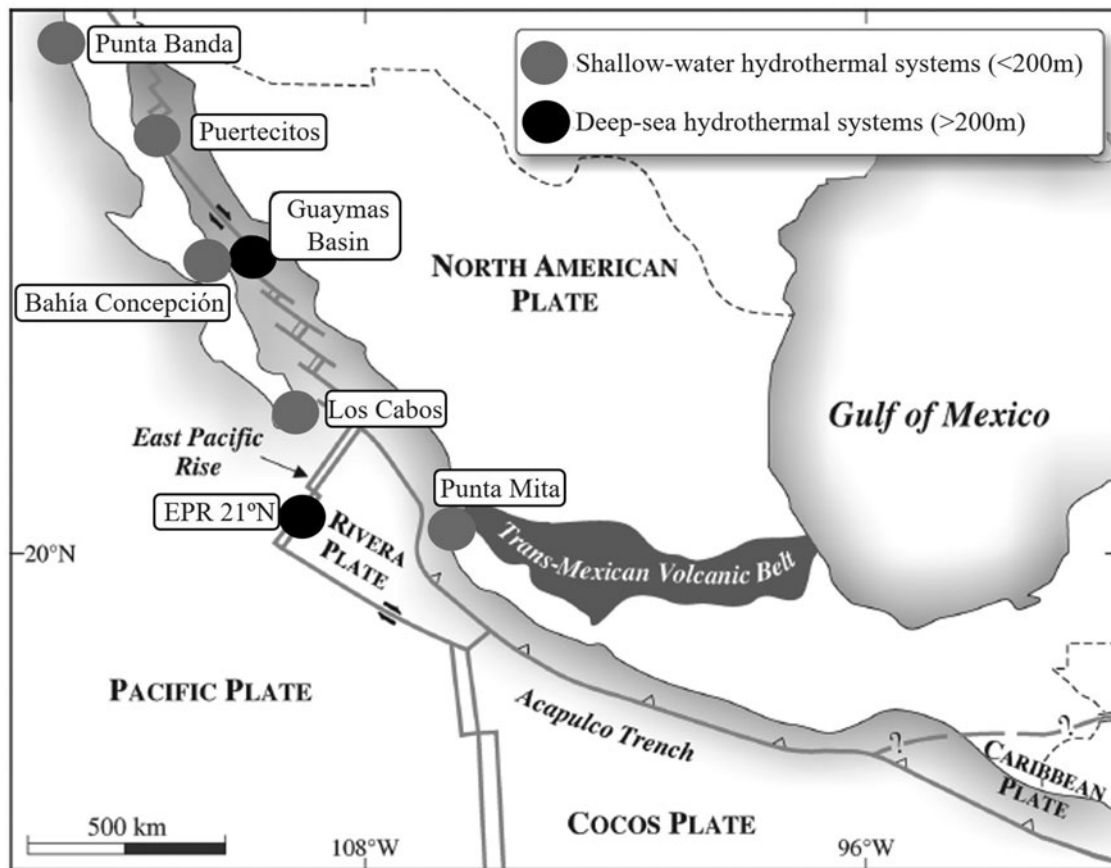
Fig. 1. Distribution of deep-sea and shallow-water hydrothermal systems in Mexico. Grey circles indicate shallow-water systems and black circles deep-sea ones. Modified map of Canet & Prol-Ledesma (2007).

1999). The lowest abundances are seen in deep-sea systems, such as the deep-sea system of the North Fiji Basin (Vanreusel *et al.*, 1997).

Regarding the fauna of shallow-water systems, the presence of species that are also found in anthropogenically contaminated environments is frequent; one of these opportunistic or highly tolerant to stressful environments species groups is the capitellid polychaetes (Tulkki, 1968; Fauchald & Jumars, 1979; Gamenick *et al.*, 1998; Tsutsumi *et al.*, 2001; Tarasov *et al.*, 2005).

The study of shallow-water hydrothermal systems can help in the understanding of various biogeochemical processes, to establish the differences between continental and submarine hydrothermal activity, in the formation of mineral deposits and the geochemical cycle of elements in the oceans (Prol-Ledesma & Canet, 2014). They are usually related to coastal volcanic activity (Tarasov *et al.*, 2005), but they can also be found on continental margins affected by active processes of tectonic extension (Prol-Ledesma & Canet, 2014), as is the case of Mexico, where a site is known in Punta Mita, Nayarit (Núñez-Cornú *et al.*, 2000; Rodríguez-Uribe *et al.*, 2020), and four sites on the coast of Baja California Peninsula: Punta Banda (Vidal *et al.*, 1978), Bahía Concepción (Prol-Ledesma *et al.*, 2004), Los Cabos (Prol-Ledesma *et al.*, 2021) and Puertecitos (Arellano-Ramirez *et al.*, 2017) (Figure 1).

In one of the five shallow-water hydrothermal systems in Mexico, in Bahía Concepción, in Baja California Sur, a study has been carried out on the benthic infauna that inhabits the sediments of this hydrothermal system (Melwani & Kim, 2008). This research focuses on the shallow-water hydrothermal system of Punta Mita (SWHSPM), located in Banderas Bay. This bay shares beaches of valuable tourist interest for the States of Nayarit and Jalisco, and the dominant ecosystem in this hydrothermal system

has not yet been determined. Therefore, this research aims to characterize the distribution of the benthic infauna that coexist in the SWHSPM.

Materials and methods

Study area

The SWHSPM is located in the area of Fisura Las Coronas (Núñez-Cornú *et al.*, 2000). Fernández de la Vega-Márquez & Prol-Ledesma (2011) reported the main geological line-ups related to this fissure. These line-ups correspond to the extensional tectonism phase of the area, which is the most recent and the cause of the Puerto Vallarta graben (Fernández de la Vega-Márquez & Prol-Ledesma, 2011). The oceanic environment of Banderas Bay is influenced by four main ocean currents: the California current, North-equatorial current, reflux from the Gulf of California and coastal ocean current from Costa Rica (Prol-Ledesma *et al.*, 2010). These currents bring arctic, subtropical and equatorial water to this bay.

In ∼400 m of the beaches of Punta Pantoque in Banderas Bay, Nayarit, Mexico, at a depth of 9 m, three sites with hydrothermal activity (Figure 2) were selected: Site 1 (S1) (20°44′54.7″N 105°28′40.6″W), Site 2 (S2) (20°44′54.8″N 105°28′40.4″W) and Site 3 (S3) (20°44′54.9″N 105°28′38.4″W). These three sites were selected because they had some of the most prominent and well-formed hydrothermal vents, compared with other sites. The distance between S1 and S2 was ∼7 m, between S2 and S3 ∼58 m, and between S3 and S1 ∼64 m.

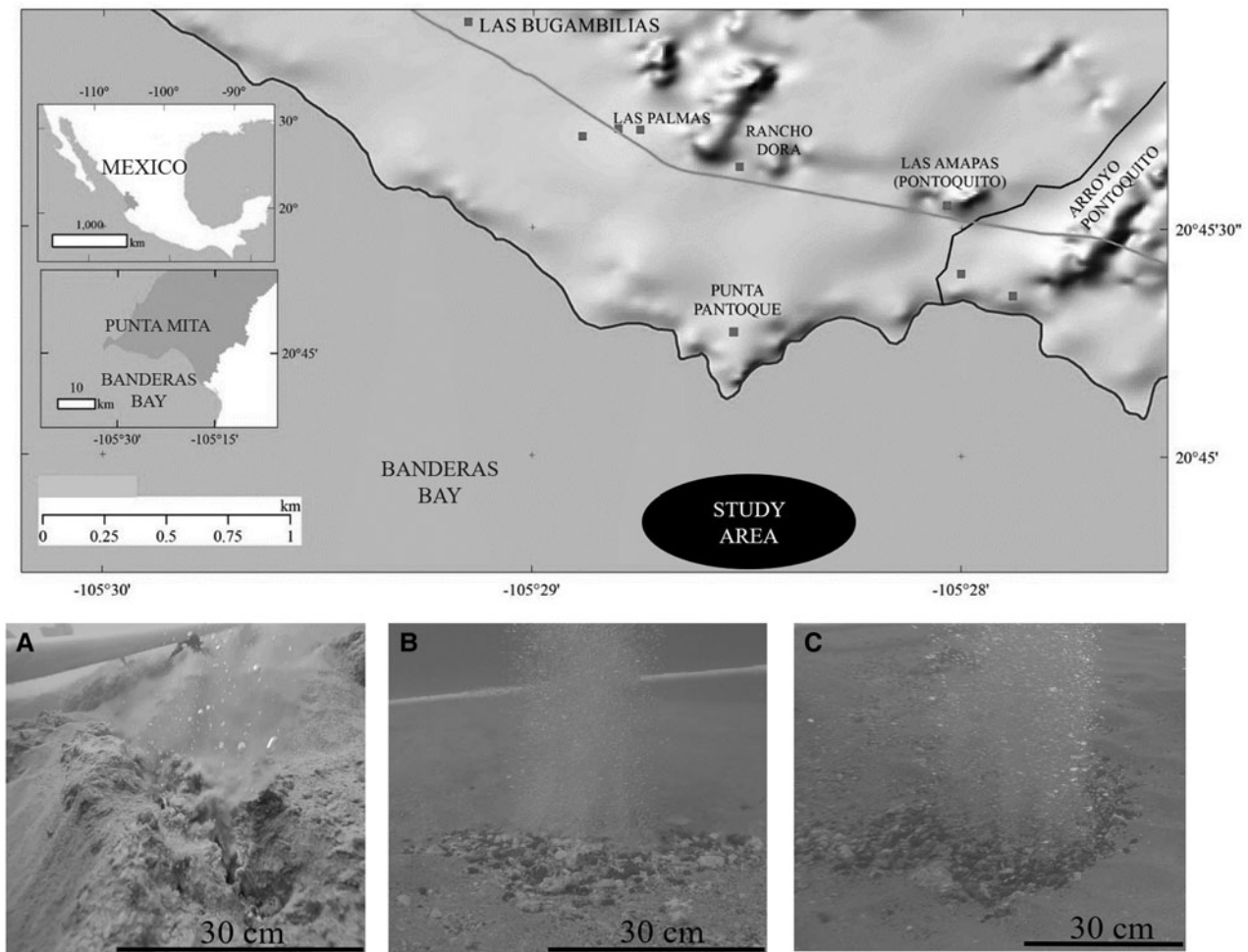Hydrothermal discharges in the SWHSPM originate mounds of calcareous tufa with Ba, Hg and Tl mineralization. These

Fig. 2. Location of the study site. The black oval indicates the study area (modified from Rodríguez-Uribe *et al.*, 2020). Pictures (A), (B) and (C) illustrate the main hydrothermal vents for each study site. (A) for site 1, (B) site 2 and (C) site 3.

mounds are formed of finely laminated calcite aggregates, and on the surfaces of these they develop arborescent textures (Canet & Prol-Ledesma, 2006). The basaltic rocks of the seabed, in the areas close to the fluid ascent ducts, are affected by hydrothermal alteration; altered basalts present plagioclase phenocrysts replaced by zeolites (heulandite and analcime) (Canet & Prol-Ledesma, 2006).

The shallow depth of the SWHSPM determines the morphology and characteristics of the accumulations of hydrothermal precipitates, since the bottom is subject to the action of waves, storms and bottom currents, the waves preventing the formation of prominent mounds (Canet *et al.*, 2000). In Figure 2A–C the main hydrothermal vents for each site are shown.

Sediment samples collection

Each study site was divided into three habitats (Figure 3), based on the bottom water temperature and the proximity to the mouth of each vent chimney. Habitat 1 (H1) is the closest to the discharge of hydrothermal fluids with an area of 0.16 m²; habitat 2 (H2) follows with 9 m², and habitat 3 (H3) is the furthest from the hydrothermal influence with an area of 36 m². In each habitat, a square area was considered. 10 × 10 cm PVC, 10 cm in diameter, plastic cores were used. On 23 November 2017, three sediment cores were collected by scuba diving in each habitat of each study site (N = 27), the approximate volume of each one was 785.40 cm³. The plastic core was inserted in the first 10 cm of the sediment or at a shallower depth if the substrate

did not allow it. The 27 sediment samples were frozen at −20°C until processing, in an 11 ft Torrey® horizontal refrigerator.

Measurements of physicochemical parameters

To record the sediment temperature of each study site (0, 3, 5 and 10 cm), a Taylor™ analogue soil thermometer, 6099N model, 1″ diameter hood, 6″ stem was used, with a temperature range from −10 to 110°C. A YSI™ Professional 1030 multiparameter probe (Pro1030) was used to record the pH, conductivity, salinity and seawater temperature at each study site.

Separation and taxonomic identification

The collected individuals were identified at the Marine Zoology Laboratory of the Instituto Tecnológico de Bahía de Banderas, Nayarit, Mexico. All the sediment cores (N = 27) were sieved in an 8″ ALCON™ brass sieve number 20 with a mesh size of 850 μm and later in a number 50 sieve of 300 μm. The individuals were fixed in 96% alcohol until identification. These individuals were observed using an Optika™ 50× stereoscopic microscope (Via Rigla, Bergamo, Italy), and were identified to the class taxonomic level, through the literature of De León-González *et al.* (2009) for polychaetes and Brusca *et al.* (2016) for the rest of the groups. The composition of the community was described with the indices of Shannon–Wiener's diversity (H'). Pielou's evenness (J') and Simpson's dominance (λ) were also calculated (Zhou *et al.*, 2017).
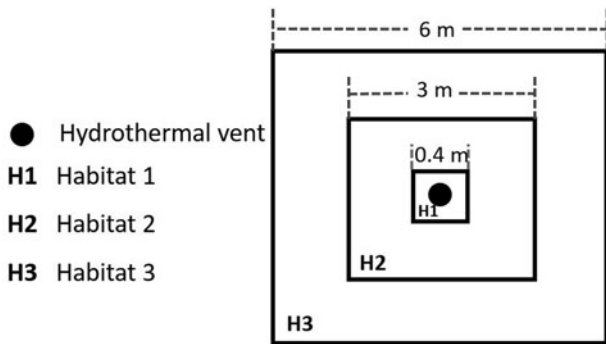
Fig. 3. Diagram showing positions of the three habitats at each study site. The black circle represents the hydrothermal vent. (H1) habitat 1, (H2) habitat 2 and (H3) habitat 3.

Organic matter content in sediment

The organic matter content was determined using the loss on ignition (LOI) method of Dean (1974), with 20 g of sediment taken from each sediment core (N = 27). An MMM™ stove, Incucell model, was used to remove humidity from samples, an Ohaus Scout™ precision balance, SPX2202 model, was used to weigh the samples, and a Thermolyne™ muffle, Furnace 48,000 model, where the treated samples were ignited at 550°C for 1 h.

Statistical analysis

A multivariate analysis of variance based on permutations (PERMANOVA) was applied in PRIMER™ + PERMANOVA version 6 software (Anderson *et al.*, 2008) with two factors, sites, and habitats, nested habitats to sites, this with fixed effects (type I
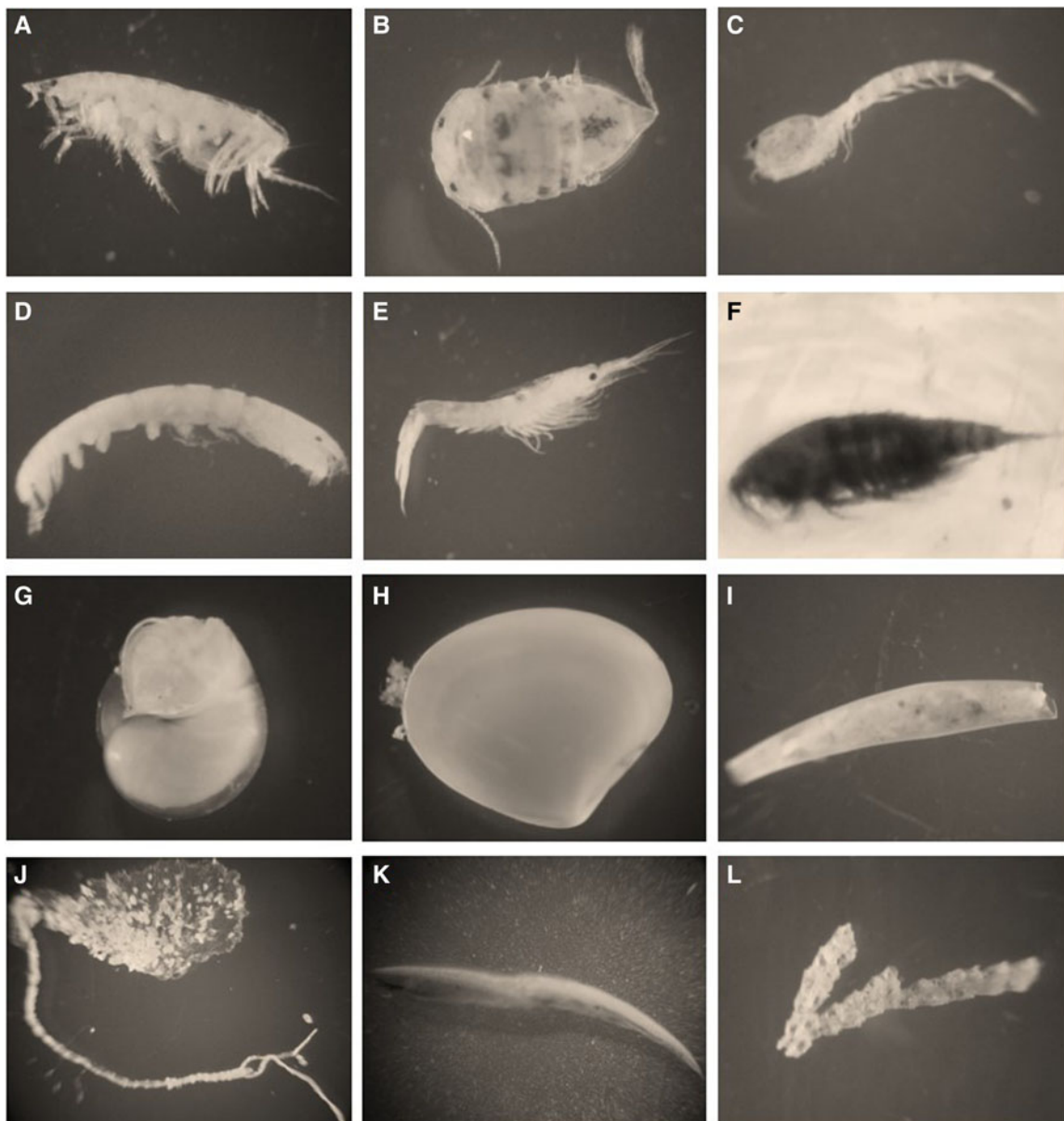
Fig. 4. Photographs of the representative individuals of each group in each taxonomic class: (A) Amphipods (Malacostraca); (B) Isopods (Malacostraca); (C) Cumaceans (Malacostraca); (D) Tanaidaceans (Malacostraca); (E) Decapods (Malacostraca); (F) Copepods (Maxillopoda); (G) Gastropods (Gastropoda); (H) Bivalves (Bivalvia); (I) Scaphopods (Scaphopoda); (J) Polychaetes (Polychaeta); (K) Amphioxus (Leptocardii); (L) Bryozoans (Stenolaemata C).
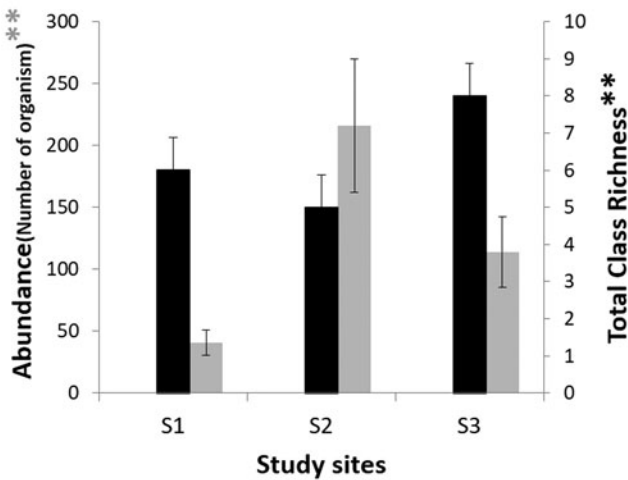
Fig. 5. Benthic infaunal total abundance at each study site indicated by the grey bars, and the total class richness is indicated by the black bars. The x-axis indicates the study sites (site 1, S1; site 2, S2; site 3, S3), and the y-axis indicates on the left side the abundance in the number of individuals, while on the right side indicates the total class richness per site.

model), to determine if there is variation in abundance at the class level of the benthic infauna of the SWHSPM. As a measure of distance, the Sorensen index was used for the abundance data, which were previously transformed with fourth root (Downing, 1979), to reduce the variation between the data, and 10,000 permutations were performed to test the statistical significance. The significance value was $P \leq 0.05$ (Anderson, 2005).

PRIMER™ + PERMANOVA version 6 software (Anderson et al., 2008) was used to perform a principal coordinate analysis (PCO) (Gower, 1966) with multiple correlations to associate the benthic infauna with the habitats and study sites. For this, the previous data matrix was used, and the similarity matrix was built with Euclidean distances.

For abiotic factors a PCO analysis was elaborated, previously a collinearity test was performed and only the most representative abiotic factors (pH, sediment temperature, water temperature, salinity and conductivity) were considered and those that explained the same as other factors were removed from the analysis. The data were normalized to Z values because they are factors of different nature (Legendre & Legendre, 2012). After this, the similarity matrix with Euclidean distance was calculated.

Results

Benthic infauna

The number of individuals were 371, corresponding to eight classes: Malacostraca, Maxillopoda, Gastropoda, Bivalvia, Scaphopoda, Polychaeta, Leptocardii and Stenolaemata. The Malacostraca class was the most abundant in the three sites with 64.69% of the total abundance, followed by the Polychaeta class with 19.14% of the total. Figure 4 shows some representative individuals for each group. At S2 the highest abundance was found (58.22%), followed by S3 (30.73%) and S1 had the lowest (11.05%). The highest class richness was found in S3 and the lowest in S2 (Figure 5 and Table 1).

The Olmstead–Tukey diagram (Figure 6) shows that the Malacostraca and Polychaeta are dominant, Gastropoda and Maxillopoda are frequent, while rare classes are Leptocardii, Scaphopoda, Stenolaemata and Bivalvia.

In each study site, H1, which is the habitat directly affected by hydrothermal activity, presents the lowest abundance values in the three sites, while the highest values were in H2 (Tables 2 and 3).

The results of the PERMANOVA analysis indicated that the number of individuals were significantly different between sites ($P = 0.0025$), while the abundance also differed between habitats and sites ($P = 0.0089$). The paired posteriori tests determined that the means of the three sites are different, S1 being different from S2 ($P = 0.0123$), S1 different from S3 ($P = 0.0403$) and S2 different from S3 ($P = 0.0056$); regarding the habitats, H1 is different from H3 ($P = 0.0017$) and there were no significant differences between H1 and H2, nor between H2 and H3 (Figure 7).

The ecological indices for this community (Table 4) shown that the value of H' was higher in S3, and S2 presented the lowest value. Meanwhile, the highest value of J' was presented at S1 and S2, and the lowest at S3. Concerning the values of λ, they had the same behaviour as the J' values.

Table 5 shows the ecological indices of the community of each habitat at each study site. In S1, it is observed that the highest value of H' was in H2 and the lowest in H1, concerning J' the highest value was in H3 and the lowest in H1, meanwhile the highest value of λ was in H1 and the lowest in H3. In S2, it is observed that the highest value of H' was in H1 and the lowest in H3, concerning J' the highest value was in H1 and the lowest in H3, meanwhile the highest value of λ was in H2 and the lowest in H1. In S3, it is observed that the highest value of H' was in H1 and the lowest in H3, concerning J' the highest

Table 1. Benthic infaunal total abundance, and richness at the taxonomic class level, of the three study sites. Site 1 (S1), site 2 (S2), and site 3 (S3)

| Phylum	Class	Study sites			Number of individuals	Abundance (%)
		S1	S2	S3		
Arthropoda	Malacostraca	27	139	74	240	64.69
	Maxillopoda	2	6	2	10	2.69
Mollusca	Gastropoda	6	18	1	25	6.74
	Bivalvia	1	4	3	8	2.16
	Scaphopoda	0	0	3	3	0.80
Annelida	Polychaeta	4	49	18	71	19.14
Chordata	Leptocardii	0	0	8	8	2.16
Bryozoa	Stenolaemata	1	0	5	6	1.62
Abundance		41	216	114	371	100%
Total class richness		6	5	8	8	

Olmstead-Tukey Diagram
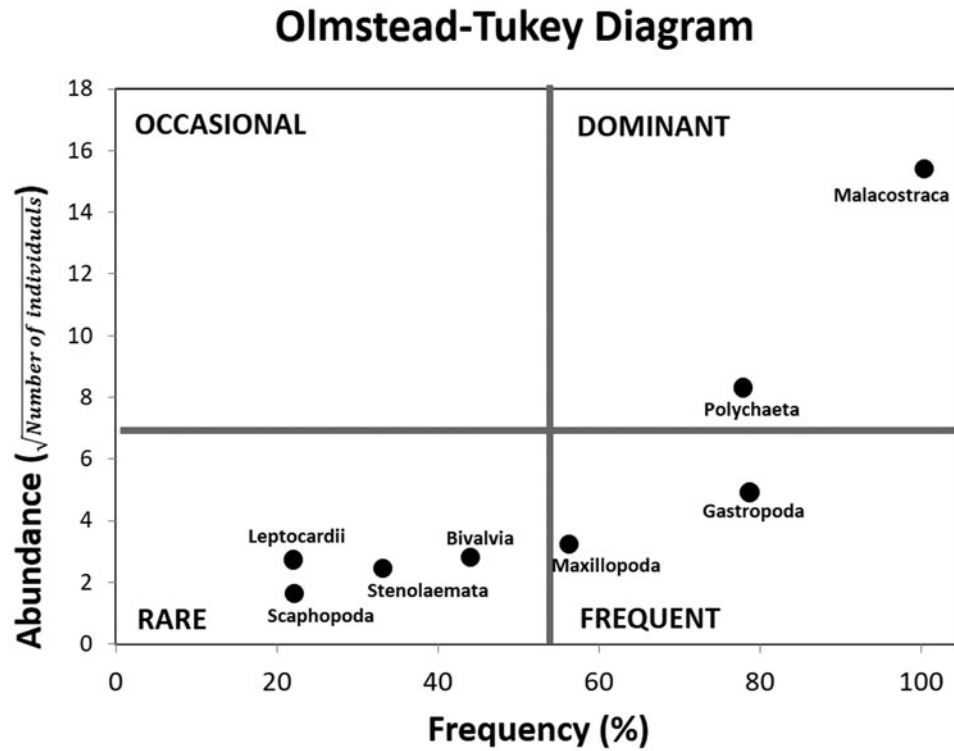
Fig. 6. Olmstead–Tukey diagram. This diagram indicates that the Malacostraca and Polychaeta classes are the dominant ones in this research, while Scaphopoda, Leptocardii, Stenolaemata and Bivalvia are the rare ones. The *x*-axis shows the frequency of the classes in percentage, and the *y*-axis is the abundance in number of individuals (transformed with a square root). Black dots locate each class on the diagram.

Table 2. The number of individuals per habitat of each study site, with their respective abundance in percentage

Site	S1		S2		S3			
Habitat	Number of individuals	Abundance (%)	Number of individuals	Abundance (%)	Number of individuals	Abundance (%)	Number of individuals	Abundance (%)
H1	9	21.95	33	15.28	9	7.89	**51**	**13.75**
H2	19	46.34	98	45.37	48	42.11	**165**	**44.47**
H3	13	31.71	85	39.35	57	50	**155**	**41.78**
Total	**41**	**100%**	**216**	**100%**	**114**	**100%**	**371**	**100%**

Site 1 (S1), site 2 (S2), site 3 (S3), habitat 1 (H1), habitat 2 (H2) and habitat 3 (H3).

Table 3. Benthic infaunal total abundance of the three study habitats, and richness at the taxonomic class level

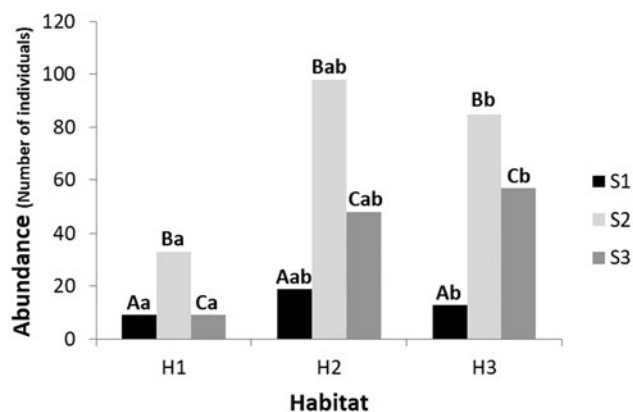| Phylum	Class	H1	H2	H3	Number of individuals	Abundance (%)
Arthropoda	Malacostraca	26	112	102	240	64.69
	Maxillopoda	1	8	1	10	2.69
Mollusca	Gastropoda	8	14	3	25	6.74
	Bivalvia	1	3	4	8	2.16
	Scaphopoda	2	1	0	3	0.80
Annelida	Polychaeta	9	23	39	71	19.14
Chordata	Leptocardii	0	3	5	8	2.16
Bryozoa	Stenolaemata	4	1	1	6	1.62
Abundance		51	165	155	371	100%
Richness		7	8	7	8	

Fig. 7. Benthic infaunal abundance by the habitat of each study site. Black bars indicate the abundance of site 1 (S1), the light grey bars of site 2 (S2), and the dark grey ones of site 3 (S3). The uppercase letters above the bars indicate significant differences between the study sites, while lowercase letters indicate significant differences between habitats at each site. Habitat 1 (H1), habitat 2 (H2) and habitat 3 (H3).

Table 4. Ecological indices

Site	Abundance (Number of individuals)	Richness (class)	J'	H'	λ
S1	41	6	0.62	1.11	0.47
S2	216	5	0.62	1.00	0.47
S3	114	8	0.58	1.20	0.46

Site 1 (S1), site 2 (S2), and site 3 (S3), Shannon–Wiener's diversity index (H'), Pielou's evenness index (J') and Simpson's dominance index (λ).

Table 5. Ecological indices of each habitat in the three study sites

Site	Habitat	Abundance (number of individuals)	Richness (class)	J'	H'	λ
S1	H1	9	3	0.62	0.68	0.63
	H2	19	5	0.70	1.13	0.44
	H3	13	4	0.77	1.07	0.43
S2	H1	33	3	0.91	1.00	0.40
	H2	98	4	0.66	0.92	0.53
	H3	85	4	0.62	0.86	0.49
S3	H1	9	5	0.89	1.43	0.28
	H2	48	7	0.59	1.14	0.46
	H3	57	4	0.58	0.80	0.58

Shannon-Wiener's diversity (H'), Pielou's evenness (J') and Simpson's dominance (λ), habitat 1 (H1), habitat 2 (H2), and habitat 3 (H3).

value was in H1 and the lowest in H3, meanwhile the highest value of λ was in H3 and the lowest in H1.

The galleries are tubes where benthic fauna are protected or hidden; 226 galleries were found of vermetids, polychaetes and tanaidaceans. The largest number of galleries were in H1 of the three study sites, with 139 galleries, meanwhile H2 had 56 galleries and H3 had 31 galleries. Figure 8 shows pictures of three representative galleries, of those found at sampling sites.

Physicochemical parameters

Table 6 shows the sediment temperature records at different depths (0, 3, 5 and 10 cm) in each habitat by study site. H1 in the three study sites recorded the highest temperatures, which increased as the depth of the sediment increased, meanwhile H3 presented the lowest values.

Four physicochemical parameters (pH, conductivity, salinity and temperature) in each habitat of each study site were recorded on two different dates (on 23 November 2017 and 4 June 2018). This was in order to observe these parameters in a cold season (November) and in a warm season (June). These parameters were recorded from 10:00–14:00 h, the means and the standard error are shown in Table 7.

In Table 7, it is observed that there is an inverse relationship concerning temperature and the rest of the parameters (pH, conductivity and salinity), that is, the higher the temperature, the lower pH, conductivity and salinity; this was observed at all three study sites. Meanwhile, H1 of the three sites recorded the highest temperatures, having a greater difference of up to 60°C with respect to H3, which is the habitat without the influence of hydrothermal activity.
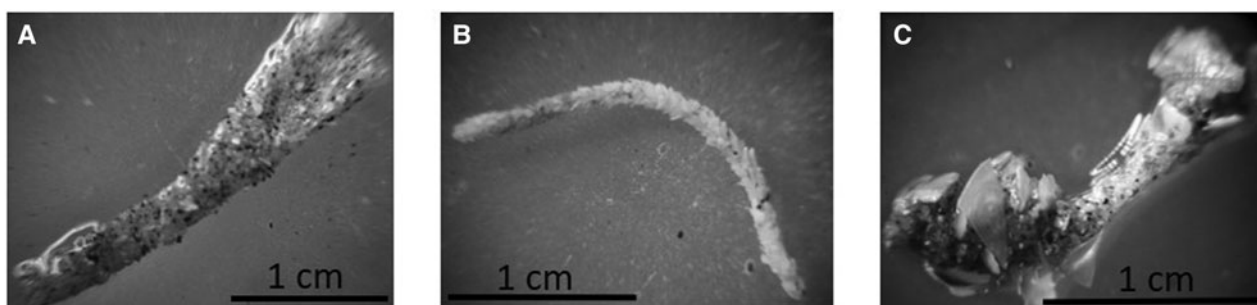

Fig. 8. Photographs of the most representative galleries of those found in the three study sites: (A) gallery found in H1 of S1, (B) gallery found in H1 of S2 and (C) gallery found in H1 of S3.

Table 6. Temperatures in °C of different depths (0, 3, 5 and 10 cm) of the sediment in each habitat of each study site

Site	S1			S2			S3		
Sediment depth (cm)	H1	H2	H3	H1	H2	H3	H1	H2	H3
0	60	32	22	40	29	23	40	30	23
3	65	33	23	68	30	23,5	62	38	24
5	70	35	24	75	32	24	75	40	26
10	82	36	24	79	35	24	84	48	28
Mean	69.25 ± 4.71	34.00 ± 0.91	23.25 ± 0.48	65.5 ± 8.8	31.5 ± 1.32	23.625 ± 0.24	65.25 ± 9.55	39.00 ± 3.7	25.25 ± 1.11

Recorded on 23 November 2017. Habitat 1 (H1), habitat 2 (H2), habitat 3 (H3), site 1 (S1), site 2 (S2) and site 3 (S3).

Organic matter

The average organic matter content found in the sediment samples for each habitat at each study site is shown in Table 8. The H3 of the three sites presented on average the lowest organic matter content (0.35 ± 0.012 g), meanwhile, H1 of the three sites presented on average the highest organic matter content (0.41 ± 0.035 g). Specifically, H1 of the S3 presented the highest content (0.048 ± 0.003 g).

Relationship of the benthic infauna with environmental parameters

The principal coordinate analysis (PCO) at the class level (Figure 9) presents an explained variation of 67.9%, in the first two axes; 38% of this variation is explained in the first axis (PCO1), while 29.9% in the second (PCO2). The explained variation in this analysis suggests the existence of an affinity of the taxonomic classes with respect to the study sites. That is, there are differences in the classes present in the study sites, which are observed in S1 and S2 concerning S3. Meanwhile, S1 and S2 are located mostly in the positive values, S3 disperses from the negative to the positive values of the first axis. Specifically, Maxillopoda, Malacostraca, Polychaeta, Bivalvia, Stenolaemata, Scaphopoda and Leptocardi classes show an affinity for S3, except the Gastropoda class. And the Stenolaemata, Scaphopoda and Leptocardi classes do not show an affinity for S1 and S2.

The PCO of environmental factors (Figure 10) presents an explained variation of 99.1% in the two first axes, where PCO1 contains 97.9% of this variation and PCO2 1.2%. This suggests an affinity of the habitat types to the environmental factors. In other words, three groups are visibly grouped, group 1: the three H1 of the three sites, group 2: the three H2 of the three sites, and group 3: the three H3 of the three sites. Besides, an inverse relationship is also observed between the water temperature and the sediment temperature, with respect to the conductivity, salinity and pH. In particular, it is observed that H1 of the three sites correlates with the highest water and sediment temperatures, H2 with intermediate values of the five environmental factors analysed, while H3 of the three sites with the lowest water and sediment temperatures, and with the highest amounts of conductivity, salinity and pH.

In Figures 9 and 10, it can be seen that the eight taxonomic classes have a greater affinity for H2 and H3 habitats at all three study sites, which are related to the lower temperatures of both the water and the sediment, as well as higher conductivity, salinity and pH measurements.

Discussion

The area of direct hydrothermal influence, called H1 of the three study sites in the SWHSPM presented the highest temperatures, both in the water and in the sediment, as well as the lowest values of pH, conductivity and salinity (these characteristics indicate the highest proportion of thermal water in the discharge and coincide with the calculated composition of the thermal end member that has high temperature, and a higher proportion of meteoric-origin water with lower salinity). This habitat has the lowest abundance of individuals and the highest abundance of galleries. Melwani & Kim (2008) reported that the high temperatures in the shallow submarine hydrothermal system of Bahía Concepción, Mexico, excluded most of the species of infauna present in the zones adjacent to this hydrothermal system. They concluded that the hydrothermal influence zone and the transition zone housed species that have strategies to manage the effect of the high temperatures present in this system, which range from 50–90°C. The aforementioned agrees with what Kamenev *et al.* (1993), Dando *et al.*

Table 7. Physicochemical parameters in each habitat of each study site (N = 72)

Habitat	pH	Conductivity (mS/cm)	Salinity (ppt)	Temperature (°C)
S1				
H1	7.635 ± 0.035	45.805 ± 0.995	18.5 ± 1.7	87.5 ± 0.5
H2	7.98 ± 0.05	54.65 ± 0.05	33.85 ± 0.75	29.05 ± 1.95
H3	8.045 ± 0.005	53.95 ± 1.45	34.05 ± 1.05	27.35 ± 0.05
S2				
H1	7.735 ± 0.025	46.515 ± 0.715	20.105 ± 1.905	86 ± 1.0
H2	8.01 ± 0.01	53.05 ± 1.955	33.9 ± 1.8	27.9 ± 2.1
H3	8.035 ± 0.005	55.05 ± 0.35	35.45 ± 0.35	26.6 ± 0.7
S3				
H1	7.665 ± 0.005	45.815 ± 0.005	17.15 ± 0.05	87.5 ± 0.5
H2	7.975 ± 0.065	51.85 ± 1.45	32.0 ± 2.9	28 ± 2.5
H3	8.065 ± 0.015	53.95 ± 1.55	35.5 ± 0.30	26.7 ± 1.1

Data were recorded on 23 November 2017 and 4 June 2018. Habitat 1 (H1), habitat 2 (H2), habitat 3 (H3), site 1 (S1), site 2 (S2) and site 3 (S3).

Table 8. Organic matter contained in the sediment samples by the habitat of each study site

Site	S1			S2			S3		
Habitat	H1	H2	H3	H1	H2	H3	H1	H2	H3
Organic matter (g)	0.38 ± 0.009	0.40 ± 0.007	0.33 ± 0.017	0.37 ± 0.003	0.34 ± 0.006	0.35 ± 0.012	0.48 ± 0.003	0.37 ± 0.009	0.37 ± 0.007

The average content is shown with its respective standard error. From the samples collected on 23 November 2017. Habitat 1 (H1), habitat 2 (H2), habitat 3 (H3), site 1 (S1), site 2 (S2) and site 3 (S3).
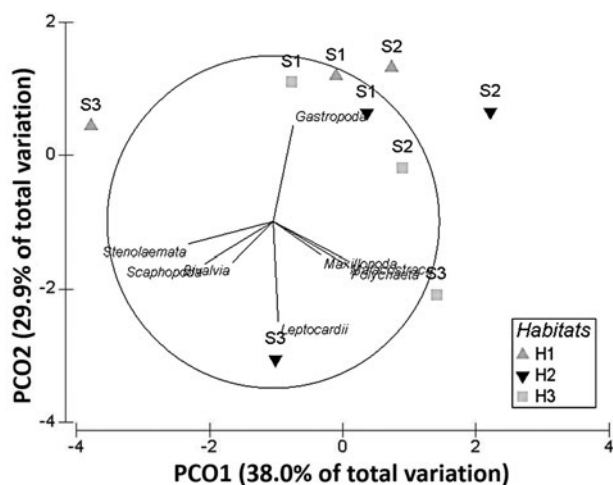

Fig. 9. Principal coordinate analysis graph. Grey triangles indicate H1, black triangles H2, grey squares H3, and the classes are labelled with their name. The x-axis explains 38% of the total variation and the y-axis explains 29.9%. Habitat 1 (H1), habitat 2 (H2), habitat 3 (H3), site 1 (S1), site 2 (S2) and site 3 (S3).

(1995) and Tarasov et al. (1999) reported, in that the macrofauna that inhabits the vicinity of a shallow hydrothermal influence must have certain types of protection from stressful physical conditions, in this case galleries.

The presence of galleries in the SWHSPM (vermetids, polychaetes and tanaidaceans) in all the habitats of the three sites makes it clear that benthic infauna has protection mechanisms against the hydrothermal influence of this hydrothermal system. We found that the highest abundances of galleries were found in H1 of the three sites, and this abundance decreased with increasing distance from the hydrothermal influence. Morri et al. (1999) suggested that the complexity generated by tubes and shells is a characteristic of fauna that inhabit shallow-water hydrothermal systems. Also, Chevaldonne et al. (1992) highlight that the use of tubes, shells and other calcareous remains can allow many species to survive the temperature differences around hydrothermal systems. The fact that the individuals of the benthic infauna in this study site build tubes or galleries may be a behavioural mechanism rather than a detoxification action for surviving in a habitat with hydrothermal activity (Gamenick et al., 1996).

In this research we are reporting that the Malacostraca and Polychaeta were the dominant classes, where the Malacostraca class includes microcrustaceans, amphipods, isopods, cumaceans, tanaidaceans and copepods. Both classes were present in the three habitats of the three study sites; these individuals have higher mobility, compared with the classes that turned out to be the rarest, i.e. Scaphopoda, Stenolaemata, Leptocardii and Bivalvia, which includes individuals with low mobility. According to Melwani & Kim (2008), mobility in species that inhabit submarine hydrothermal systems provides them with a strategy for survival when protection, tolerance or detoxification mechanisms are absent. Although swimmers have a more mobile strategy, other sediment-dwelling groups can also exploit mobility, either burrowing or crawling. The textural composition of the sediments of S1, S2 and S3 has been reported by Rodríguez-Uribe et al. (2020), ~2 weeks apart, they collected the samples on 13 December 2017, where the very fine sand was the dominant grain size in the three sites.

The presence of the Leptocardii class was not recorded in any hydrothermal influence area. This class includes the
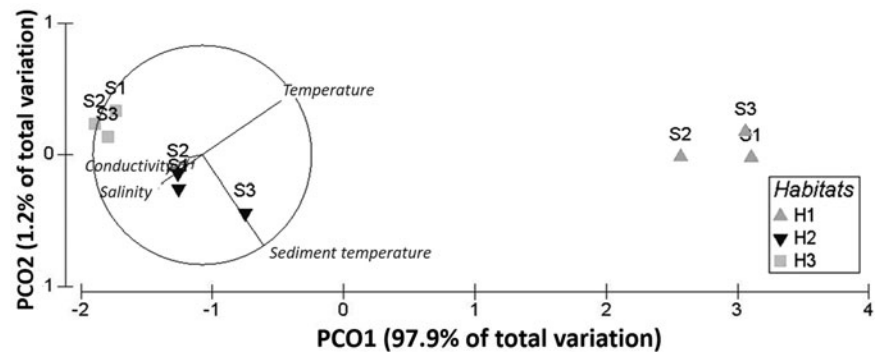
Fig. 10. Principal coordinate analysis graph. Grey triangles indicate H1, black triangles H2, grey squares H3, and the environmental factors are labelled with their name. The *x*-axis explains 97.9% of the total variation and the *y*-axis explains 1.2%. Habitat 1 (H1), habitat 2 (H2), habitat 3 (H3), site 1 (S1), site 2 (S2) and site 3 (S3).

cephalochordates; the adults are occasional swimmers since they prefer the benthic substrate for the locomotion, where they spend most of their time filtering their food (Garcia-Fernàndez & Benito-Gutiérrez, 2009). Most probably the absence of these is due to the high temperatures of the sediment, since cephalochordates generally inhabit shallow marine waters near the coast (Del Moral-Flores *et al.*, 2016; Galván-Villa *et al.*, 2017).

The three H1 of the three study sites presented the lowest abundances of individuals and a benthic infauna community very similar to that found in the habitats farthest from the hydrothermal influence (H2 and H3), except for the Leptocardii class. This result is attributed to the stressful conditions of the habitat with the direct hydrothermal influence of the SWHSPM. Couto *et al.* (2015) carried out a review of the papers on flora and fauna present in shallow-water hydrothermal systems in the Azores Islands in Portugal, and found that the individuals within these hydrothermal systems are similar to those found in the coastal and submarine areas of the archipelago (Cardigos *et al.*, 2005), but with lower abundances. Also, in the comparative study of Marques-Mendes (2008) between the benthos communities affected by hydrothermal activity and another site without this activity, he concludes that the community present in the hydrothermal system has almost the same composition as the communities without hydrothermal activity, but with less abundance.

Hall-Spencer *et al.* (2008) reported how acidification caused by gas discharges in cold vent areas off Ischia in Italy significantly decreased the abundances of certain species of coralline algae, where the pH levels recorded were the lowest in the study (7.4–7.5). On the other hand, in the study of Álvarez-Castillo *et al.* (2018) carried out in the Wagner and Consag basins, Gulf of California, Mexico, where more than 300 sites with CO_2 bubbles rising to the surface have been reported, they reported that lower meiofauna densities were also related to lower pH levels (6.06–6.48). The aforementioned is in agreement with our results since the lowest pH levels (7.64–7.74) were recorded in the areas of direct influence of the SWHSPM, which has been associated with a lower abundance of infauna in those study areas.

Quite contrary to the chemical conditions in SWHSPM, in sulphurous hydrothermal systems, the abundances of polychaetes are often increased, due to the high tolerance to hydrogen sulphide and anoxia (Melwani & Kim, 2008). Thus, in White Point hydrothermal vents (San Pedro Bay, USA) hydrogen sulphide was the most influential variable between the zones with and without hydrothermal activity, therefore the polychaetes *Apoprionospio pygmaea* and *Prionospio heterobranchia*, both of the family Spionidae were the most abundant in this site (Melwani & Kim, 2008). Nereid and capitellid polychaetes have already been documented to be able to tolerate long-term sulphide exposure (Vismann, 1990). The sulphidic habitats have been proposed as ideal refuges for animals capable of resisting sulphide toxicity (Bagarinao, 1992). It has also been reported that certain genera

of algae have been shown to be resistant to natural amounts of pCO_2 (Hall-Spencer *et al.*, 2008), for example, *Caulerpa*, *Cladophora*, *Asparagopsis, Dictyota* and *Sargassum*, and that they are directly related to low pH levels as reported in the cold vent areas off Ischia in Italy (Hall-Spencer *et al.*, 2008). Some of these algal species include invasive alien species that have already begun to alter shallow marine ecosystems worldwide (Boudouresque & Verlaque, 2002; Hall-Spencer *et al.*, 2008).

The high temperature (89°C) of the SWHSPM has an inverse relationship with pH and salinity, thus being the environmental factor that structures the benthic infaunal community, since it was the only environmental variable that differed significantly between the three habitats of the three study sites. Despite this, members of the communities adjacent to this hydrothermal system are not completely excluded, since the only class that does not occur in the area of hydrothermal influence is the Leptocardii, because they do not tolerate high sediment temperatures, while the remaining seven classes are present, only in lower abundances. In addition, the benthic individuals present in the hydrothermal influence area use protection strategies against extreme conditions, evidenced by the high abundance of galleries found in this habitat. The temperature and pH levels in the SWHSPM make this site a place with great potential for the study of ocean acidification, due to its shallow depth and proximity to the beach.

References

Álvarez-Castillo L, Hermoso-Salazar M, Estradas-Romero A, Rivas G and Prol-Ledesma RM (2018) Composition and spatial distribution of the meiofauna in the Wagner and Consag basins, Gulf of California, Mexico. *Cahiers de Biologie Marine* **59**, 245–256.

Anderson MJ (2005) *PERMANOVA: A FORTRAN Computer Program for Permutational Multivariate Analysis of Variance.* New Zealand: Department of Statistics, University of Auckland.

Anderson M, Gorley RN and Clarke KR (2008) *PERMANOVA + for PRIMER User Manual*, vol. 1. Plymouth, UK: Prim Ltd Regist, 1:218.

Arellano-Ramirez Y, Kretzschmar TG and Hernandez-Martinez R (2017) Water-rock-microbial interactions in the hydrothermal spring of Puertecitos, Baja California, Mexico. *Procedia Earth and Planetary Science* 17, 865–868.

Bagarinao T (1992) Sulfide as an environmental factor and toxicant: tolerance and adaptations in aquatic organisms. *Aquatic Toxicology* 24, 21–62.

Boudouresque CF and Verlaque M (2002) Biological pollution in the Mediterranean Sea: invasive *vs* introduced macrophytes. *Marine Pollution Bulletin* 44, 32–38.

Brusca RC, Moore W and Shuster SM (2016) *Invertebrates*. 3rd edition. Oxford: Oxford University Press.

Canet C and Prol-Ledesma RM (2006) Procesos de mineralización en manantiales hidrotermales submarinos someros. Ejemplos en México. *Boletín de La Sociedad Geológica Mexicana* 58, 83–102.

Canet C and Prol-Ledesma RM (2007) Mineralizing processes at shallow submarine hydrothermal vents: examples from Mexico. *Special Paper of the Geological Society of America* 422, 359–376.

Canet C, Prol-Ledesma RM and Melgarejo JC (2000) El sistema hidrotermal de Punta Mita (México): un ejemplo de depósito exhalativo submarino actual. *Cadernos Lab. Xeolóxico de Laxe* 25, 325–327.

Cardigos F, Colaço A, Dando PR, Ávila SP, Sarradin PM, Tempera F, Conceição P, Pascoal A and Santos RS (2005) Shallow water hydrothermal vent field fluids and communities of the D. João de Castro Seamount (Azores). *Chemical Geology* 224, 153–168.

Chevaldonne P, Desbruyeres D and Childress JJ (1992) Some like it hot and some even hotter. *Nature* 359, 593–594.

Couto RP, Rodrigues AS and Neto AI (2015) Shallow-water hydrothermal vents in the Azores (Portugal). *Journal of Integrated Coastal Zone Management* 15, 495–505.

Dando PR, Hughes JA, Leahy Y, Niven SJ, Taylor LJ and Smith C (1995) Gas venting rates from submarine hydrothermal areas around the island of Milos, Hellenic Volcanic Arc. *Continental Shelf Research* 15, 913–929.

Dean WE (1974) Determination of carbonate and organic matter in calcareous sediments and sedimentary rocks by loss on ignition: comparison with other methods. *Journal of Sedimentary Petrology* 44, 242–248.

De León-González JA, Bastida-Zavala JR, Carrera-Parra F, García-Garza ME, Peña-Rivera A, Salazar-Vallejo SI and Solis-Weiss V (2009) *Poliquetos (Annelida: Polychaeta) de México y América Tropical*. (U. A. de N. L. Dirección de Publicaciones, Ed.). Mexico.

Del Moral-Flores LF, Guadarrama-Martínez MA and Flores-Coto C (2016) Composición taxonómica y distribución de los cefalocordados (Cephalochordata: Amphioxiformes) en México. *Latin American Journal of Aquatic Research* 44, 497–503.

Downing JA (1979) Aggregation, transformation, and the design of benthos sampling programs. *Journal of the Fisheries Research Board of Canada* 36, 1454–1463.

Engel BE, Hallock P, Price RE and Pichler T (2015) Shell dissolution in larger benthic foraminifers exposed to pH and temperature extremes: results from an in situ experiment. *Journal of Foraminiferal Research* 45, 190–203.

Fabricius KE, Langdon C, Uthicke S, Humphrey C, Noonan S, De'ath G, Okazaki R, Muehllehner N, Glas MS and Lough JM (2011) Losers and winners in coral reefs acclimatized to elevated carbon dioxide concentrations. *Nature Climate Change* 1, 165–169.

Fauchald K and Jumars PA (1979) The diet of worms: a study of polychaete feeding guilds. *Marine Biology: An Annual Review* 17, 193–284.

Fernández de la Vega-Márquez T and Prol-Ledesma RM (2011) Imágenes landsat TM y modelo digital de elevación para la identificación de lineamientos y mapeo litológico en punta mita (México). *Boletin de La Sociedad Geologica Mexicana* 63, 109–118.

Galván-Villa CM, Ríos-Jara E and Ayón-Parente M (2017) Nuevos registros de la lanceta de California branchiostoma californiense (Cephalochordata: Branchiostomidae) de la costa Pacífica de México. *Revista Mexicana de Biodiversidad* 88, 995–998.

Gamenick I, Abbiati M and Giere O (1998) Field distribution and sulphide tolerance of *Capitella capitata* (Annelida: Polychaeta) around shallow water hydrothermal vents off Milos (Aegean Sea). A new sibling species? *Marine Biology* 130, 447–453.

Gamenick I, Jahn A, Vopel K and Giere O (1996) Hypoxia and sulphide as structuring factors in a macrozoobenthic community on the Baltic Sea shore: colonisation studies and tolerance experiments. *Marine Ecology Progress Series* 144, 73–85.

Garcia-Fernàndez J and Benito-Gutiérrez È (2009) It's a long way from amphioxus: descendants of the earliest chordate. *BioEssays* 31, 665–675.

Garrison T and Ellis R (2016) *Oceanography: An Invitation to Marine Science*, 9th edition. Boston, MA: Cengage Learning.

Gower JC (1966) Some distance properties of latent root and vector methods used in multivariate analysis. *Biometrika* 53, 325–338.

Hall-Spencer JM, Rodolfo-Metalpa R, Martin S, Ransome E, Fine M, Turner SM, Rowley SJ, Tedesco D and Buia MC (2008) Volcanic carbon dioxide vents show ecosystem effects of ocean acidification. *Nature* 454, 96–99.

Kamenev GM, Fadeev VI, Selin NI, Tarasov VG and Malakhov VV (1993) Composition and distribution of macro- and meiobenthos around sublittoral hydrothermal vents in the Bay of Plenty, New Zealand. *New Zealand Journal of Marine and Freshwater Research* 27, 407–418.

Legendre P and Legendre L (2012) *Numerical Ecology. Developments in Environmental Modelling*. Amsterdam: Elsevier B.V.

Marques-Mendes AR (2008) *Influência Das Fontes Hidrotermais Marinhas De Baixa Profundidade Na Composição Das Comunidades De Meiofauna*. Ponta Delgada, Azores: Universidade Dos Açores.

Melwani AR and Kim SL (2008) Benthic infaunal distributions in shallow hydrothermal vent sediments. *Acta Oecologica* 33, 162–175.

Morri C, Blanchi CN, Cocito S, Peirano A, De Biase AM, Aliani S, Pansini M, Boyer M, Ferdeghini F, Pestarino M and Dando P (1999) Biodiversity of marine sessile epifauna at an Aegean island subject to hydrothermal activity: Milos, eastern Mediterranean Sea. *Marine Biology* 135, 729–739.

Núñez-Cornú FJ, Prol-Ledesma RM, Cupul-Magaña A and Suárez-Plascencia C (2000) Near shore submarine hydrothermal activity in Bahia Banderas, western Mexico. *Geofisica Internacional* 39, 171–178.

Price RE and Giovannelli D (2017) A review of the geochemistry and microbiology of marine shallow-water hydrothermal vents. In *Reference Module in Earth Systems and Environmental Sciences*. Amsterdam: Elsevier, p. 30.

Prol-Ledesma RM and Canet C (2014) Evaluación y explotación de los recursos geotérmicos del océano. In Low Pfeng AM and Recagno EP (eds), *La Frontera Final: el Océano Profundo*. Mexico: SEMARNAT-INECC, pp. 11–30.

Prol-Ledesma RM, Canet C, Torres-Vera MA, Forrest MJ and Armienta MA (2004) Vent fluid chemistry in Bahía Concepción coastal submarine hydrothermal system, Baja California Sur, Mexico. *Journal of Volcanology and Geothermal Research* 137, 311–328.

Prol-Ledesma RM, Canet C, Villanueva-Estrada RE and Ortega-Osorio A (2010) Morphology of pyrite in particulate matter from shallow submarine hydrothermal vents. *American Mineralogist* 95, 1500–1507.

Prol-Ledesma RM, Carrillo De La Cruz JL, Torres-Vera MA and Estradas-Romero A (2021) High heat flow at the SW passive margin of the Gulf of California. *Terra Nova* 2, 1–8.

Prol-Ledesma RM, Dando PR and de Ronde CEJ (2005) Special issue on 'shallow-water hydrothermal venting'. *Chemical Geology* 224, 1–4.

Reeves EP, Seewald JS, Saccocia P, Bach W, Craddock PR, Shanks WC, Sylva SP, Walsh E, Pichler T and Rosner M (2011) Geochemistry of hydrothermal fluids from the PACMANUS, Northeast Pual and Vienna Woods hydrothermal fields, Manus Basin, Papua New Guinea. *Geochimica et Cosmochimica Acta* 75, 1088–1123.

Rodríguez-Uribe MC, Núñez-Cornú FJ, Chávez-Dagostino RM and Trejo-Gómez E (2020) Granulometric analysis of shallow vents sediments at Banderas Bay (Mexico). *Journal of Marine Science and Engineering* 8, 1–11.

Tarasov VG (1999) *The Coastal Ecosystems and Shallow-Water Hydrothermal Venting*. Vladivostok: Russian: Dalnauka Press.

Tarasov VG, Gebruk AV, Mironov AN and Moskalev LI (2005) Deep-sea and shallow-water hydrothermal vent communities: two different phenomena? *Chemical Geology* 224, 5–39.

Tarasov VG, Gebruk AV, Shulkin VM, Kamenev GM, Fadeev VI, Kosmynin VN, Malakhov VV, Starynin DA and Obzhirov AI (1999) Effect of shallow-water hydrothermal venting on the biota of Matupi Harbour (Rabaul Caldera, New Britain Island, Papua New Guinea). *Continental Shelf Research* 19, 79–116.

Thiermann F, Windoffer R and Giere O (1994) Selected meiofauna around shallow water hydrothermal vents off Milos (Greece): ecological and ultrastructural aspects. *Vie et Milieu* 44, 215–226.

Tsutsumi H, Wainright S, Montani S, Saga M, Ichihara S and Kogure K (2001) Exploitation of a chemosynthetic food resource by the polychaete Capitella sp. I. *Marine Ecology Progress Series* 216, 119–127.

Tulkki P (1968) Effect of pollution on the benthos off Gothenburg. *Helgoländer Wissenschaftliche Meeresuntersuchungen* **17**, 209–215.

Vanreusel A, Van Den Bossche I and Thiermann F (1997) Free-living marine nematodes from hydrothermal sediments: similarities with communities from diverse reduced habitats. *Marine Ecology Progress Series* **157**, 207–219.

Vidal VMV, Vidal FV and Isaacs JD (1978) Coastal submarine hydrothermal activity off Northern Baja California. *Journal of Geophysical Research* **83**, 1757–1774.

Vismann B (1990) Sulfide detoxification and tolerance in *Nereis* (*Hediste*) *diversicolor* and *Nereis* (*Neanthes*) *virens* (Annelida: Polychaeta). *Marine Ecology Progress Series* **59**, 229–238.

Yang K and Scott SD (1996) Possible contribution of a metal-rich magmatic fluid to a sea-floor hydrothermal system. *Nature* **383**, 420–423.

Zhou B, Wang T, Li Y and Bralts V (2017) Effects of microbial community variation on bio-clogging in drip irrigation emitters using reclaimed water. *Agricultural Water Management* **194**, 139–149.